

Article

Temporal Characteristics and Sources of PM_{2.5} in Porto Velho of Amazon Region in Brazil from 2020 to 2022

Yu-Woon Jang¹ and Gi-Woong Jung^{2,*}

¹ Institute of Latin American Studies, Hankuk University of Foreign Studies, Seoul 02450, Republic of Korea; glarecloud@daum.net

² Center for International Area Studies, Hankuk University of Foreign Studies, Seoul 02450, Republic of Korea

* Correspondence: jgw@hufs.ac.kr; Tel.: +82-2-2173-3181

Abstract: Our study analyzed PM_{2.5} concentrations in Porto Velho, Rondônia, during the April 2020 and October 2022 wildfire seasons. This study aimed to evaluate the temporal characteristics of PM_{2.5} and the influence of long-distance pollution sources. Using PurpleAir data, we found that the average PM_{2.5} concentration was $17.7 \pm 24.0 \mu\text{g m}^{-3}$, with significant spikes in August. PM_{2.5} concentrations decreased during the day but rose from nighttime to morning. The PM_{2.5} concentration was observed to be distributed at a high level of $36.3 \pm 31.1 \mu\text{g m}^{-3}$ in slow westerly winds. Moreover, even in the dominant northerly wind conditions, a similarly high concentration of PM_{2.5} was detected, measuring at $33.2 \pm 28.3 \mu\text{g m}^{-3}$. Air masses mainly originated from northeastern, southeastern, and southern regions, passing through Paraguay and Bolivia. Furthermore, PM_{2.5} in Porto Velho was influenced by Brazil's northern and Central-West areas. To meet the Sustainable Development Goal (SDG) Indicator 11.6.2 for clean air, it is recommended that wildfires in Porto Velho's northern and western regions be reduced, and more robust deforestation policies are needed in areas with long-distance pollution sources.

Keywords: Porto Velho; wildfire; PM_{2.5}; SDG Indicator 11.6.2



Citation: Jang, Y.-W.; Jung, G.-W.

Temporal Characteristics and Sources of PM_{2.5} in Porto Velho of Amazon Region in Brazil from 2020 to 2022. *Sustainability* **2023**, *15*, 14012. <https://doi.org/10.3390/su151814012>

Academic Editor: Konstantinos Dimitriou

Received: 7 August 2023

Revised: 16 September 2023

Accepted: 19 September 2023

Published: 21 September 2023



Copyright: © 2023 by the authors. Licensee MDPI, Basel, Switzerland. This article is an open access article distributed under the terms and conditions of the Creative Commons Attribution (CC BY) license (<https://creativecommons.org/licenses/by/4.0/>).

1. Introduction

The Amazon rainforest plays a pivotal role as a carbon sink, absorbing greenhouse gases and thereby regulating climate change [1,2]. However, intentional wildfires are set in the Amazon during the dry season to clear land for pasture and agriculture [3,4]. These wildfires are significant carbon emission sources, producing carbon aerosols that amplify the impacts of climate change [5–7]. Exacerbated climate change conditions, characterized by more frequent droughts and longer dry seasons, further amplify wildfire occurrences [8].

Wildfires have the potential to adversely affect the health of residents both in the immediate vicinity of the fire outbreak and in downwind regions through long-range transport mechanisms [9–11]. Notably, PM_{2.5} emissions from wildfires are known to be more harmful than those originating from fossil fuels, and the increase in wildfires correlates with a rise in atmospheric PM_{2.5} concentrations [11–13]. Attention to PM_{2.5} concentrations is crucial as they influence respiratory ailments, cardiovascular diseases, and cognitive function decline in individuals [14–16]. Thus, elevated levels of PM_{2.5} run counter to Sustainable Development Goal (SDG) 11.6.2, which aims to reduce adverse health impacts from air pollutants, including fine particulate pollution [17,18]. Air quality enhancement through PM_{2.5} reduction is pivotal to achieving sustainable development objectives.

An increase in the daily average concentration of wildfire-related PM_{2.5} by $10 \mu\text{g m}^{-3}$ led to a 3.1% rise in mortality rate, whereas an increase in the annual or biennial average PM_{2.5} concentration by $1 \mu\text{g m}^{-3}$ resulted in a 0.14% or 2% increase in mortality rate, respectively [10,15,19,20]. On the other hand, a decrease in PM_{2.5} levels by $10 \mu\text{g m}^{-3}$, or

meeting the WHO recommended level of $10 \mu\text{g}/\text{m}^3$, led to an increase in life expectancy [21,22]. While air quality improvement policies focus on reducing $\text{PM}_{2.5}$ and other pollutants in major urban areas, the effect of local and distant wildfires on urban $\text{PM}_{2.5}$ concentrations cannot be ignored [13].

Research related to $\text{PM}_{2.5}$ resulting from wildfires has also been conducted in the Amazon region [23,24]. Wildfire-induced $\text{PM}_{2.5}$ concentrations have been exceptionally high in the central-western parts of Brazil, affecting the health of children, women, and the elderly aged 65 and over [15,20,25,26]. Porto Velho, situated in the central-western Amazon of Brazil, is the capital of the Rondônia state and is home to approximately 500,000 residents. Rondônia is notably among the regions experiencing the most severe deforestation within Brazil. In the Amazon area, 80% of $\text{PM}_{2.5}$ emissions are attributed to deforestation [27]. Therefore, understanding the impact of wildfires stemming from deforestation on the sustainable well-being of the region's inhabitants is of paramount importance.

Previous studies have used satellite data and modeling techniques, presenting challenges in assessing specific areas in the Amazon [20,25,28,29]. Recent observational data for $\text{PM}_{2.5}$ in the region are outdated, and the sampling period for $\text{PM}_{2.5}$ exceeded two days, limiting the understanding of the diurnal variation of $\text{PM}_{2.5}$ from wildfires [25,27].

This research utilizes hourly average $\text{PM}_{2.5}$ data from PurpleAir. It aims to evaluate the temporal characteristics of $\text{PM}_{2.5}$ in conjunction with meteorological data during wildfire periods and the influence of long-distance pollution sources. Through this, we expect to contribute to the sustainable goal of clean atmospheric quality (SDG Indicator 11.6.2) for the area's residents.

2. Methods

2.1. $\text{PM}_{2.5}$ and Meteorological Data

In the Amazon region, inclusive of the Porto Velho area, there are no regulatory-grade monitors. Instead, hourly measurement data regarding particulate matter are acquired using PurpleAir's Low-Cost Sensor (PALCS). This study utilized $\text{PM}_{2.5}$ data provided by PurpleAir (<https://www2.purpleair.com/> (accessed on 30 July 2023)) from April 2020 to October 2022. The data can be downloaded using the PurpleAir Data Download Tool. The PALCS system comprises two channels, labeled as A and B. Utilizing these two channels, it simultaneously measures the mass concentrations of PM_1 , $\text{PM}_{2.5}$, and PM_{10} , along with particle counts for sizes of 0.3, 0.5, 1.0, 2.5, 5.0, and $10.0 \mu\text{m}$. Additionally, the system records meteorological variables, including temperature, relative humidity, and atmospheric pressure. Data from both channels are utilized for the purpose of data verification. It is notably employed in areas experiencing extensive wildfires [30–32]. Ardon-Dryer et al. [23] found a good agreement (75% of the comparison had a $R^2 > 0.8$) between regulatory-grade monitors and low-cost sensors in wildfire areas. To conduct Quality Control (QC) in our research, we first calculated the differences and relative percentiles of the raw data, precisely the PA_cf1 measurements, obtained from channels A and B. Adhering to the QC criteria proposed by the U.S. EPA, only data exhibiting a difference of $5 \mu\text{g m}^{-3}$ or less, or a relative percentile of 70% or less, were utilized in our analysis [33]. Consequently, 1.5% of the data were excluded from this study. In studies on wildfire-affected areas, there have been cases where data removal rates through QC for Channel A and Channel B of PALCS were 2.6% and 4%, respectively [33,34]. The correlation of $\text{PM}_{2.5}$ between Channels A and B showed a good fit ($R^2 = 0.99$). Additionally, the Root Mean Square Error (RMSE) showed a 2.8% improvement following QC.

Secondly, an issue was identified with the PALCS's final data, denoted as PA_atm , which appeared to overestimate measurements compared to regulatory-grade monitors [35]. The U.S. EPA has proposed Equation (1) to adjust the PA_atm data, leveraging the results from regulatory-grade monitors and incorporating $\text{PM}_{2.5}$ concentration and relative humidity [33].

$$\text{PM}_{2.5} = \text{PA_cf1} \times 0.524 - 0.0862 \times \text{RH} + 5.75 \quad (1)$$

where $PM_{2.5}$ is the corrected PurpleAir sensor mass concentration, PA_cf1 is the raw data of $PM_{2.5}$ concentration measured with PALCS, and RH is the relative humidity.

In this research, we also adopted this method, rectifying the excessive measurements of PALCS (Equation (2))

$$PM_{2.5} = 0.762 \times PA_atm - 1.704 \quad (2)$$

Meteorological data (wind speed, wind direction, temperature, relative humidity, visibility) were sourced “from timeanddate website (<https://www.timeanddate.com> (accessed on 30 July 2023))”. The mixing height data were determined using the Vmixing program of the NOAA’s Lagrangian integrated trajectory (Hysplit4 model, <https://www.ready.noaa.gov/HYSPLIT.php> (accessed on 30 July 2023)). The data utilized in the Vmixing program were based on the GDAS1 dataset (<https://www.ready.noaa.gov/data/archives/gdas1/> (accessed on 30 July 2023)), which provides reanalysis data at a 1° by 1° resolution.

2.2. Wildfire Information

Visible Infrared Imaging Radiometer Suite (VIIRS) was developed to enhance the capabilities of the Advanced Very-High Resolution Radiometer (AVHRR) [36]. Currently, VIIRS’s active fire detection products are available in both 750 m and 375 m spatial resolutions [37]. The 375 m resolution product from VIIRS offers improved sensitivity to smaller fires and boasts a higher rate of detection [36]. The VIIRS data were downloaded from the BDQEUMADAS website, which is operated by the Brazilian National Institute for Space Research under the Ministry of Science, Technology, and Innovation (<http://terrabrasilis.dgi.inpe.br/queimadas/bdqueimadas> (accessed on 30 July 2023)). The data are based on the 375 m resolution Visible Infrared Imaging Radiometer Suite (VIIRS) dataset.

2.3. Back-Trajectory Analysis

To investigate the long-range transport of $PM_{2.5}$, the Hysplit4 model was employed to conduct a back trajectory analysis of the air inflow at a height of 500 m above the measurement site over 72 h (<https://www.ready.noaa.gov/hypub-bin/trajtype.pl?runtype=archive> (accessed on 30 July 2023)).

The meteorological data used for the back trajectory transport were from the GFS (Global Forecast Model) at a resolution of 0.25° by 0.25° . Additionally, to determine the long-range wildfire regions contributing to the $PM_{2.5}$ concentrations in the Porto Velho area, we applied the potential source contribution function (PSCF) and concentration-weighted trajectory (CWT) models, leveraging trajectory analysis data. The Openair package in the R program was used to analyze PSCF, CWT, and cluster analysis in order to evaluate long-range emission sources [27].

2.4. PSCF Model

The PSCF model calculates a conditional probability, assessing the chance that a trajectory moving through a particular geographic grid cell will lead to a concentration surpassing a defined threshold (in this study, 24 h $PM_{2.5}$ standard $50 \mu\text{g m}^{-3}$) when it reaches the receptor site (Equation (3)).

$$PSCF_{ij} = m_{ij}/n_{ij} \quad (3)$$

where m_{ij} denotes the count of trajectory points that traverse the ij grid cell when the concentration at the site of Porto Velho exceeds a specific criterion, and n_{ij} represents the total number of air masses that enter the i th and j th cells over the study period.

The domain was defined with a latitude range from 26 S to 1 N and a longitude range from 45 S to 73 S, with a grid size set at 0.5° by 0.5° . While grids with high probability values ($PSCF_{ij}$) can be identified as emission sources, those with limited trajectories can exhibit significant uncertainties. To address this limitation, a weighting factor (W_{ij}) can

be employed. In this study, the Openair package in R, which we utilized, incorporates a weighting factor as described in Equation (4) [38]. A weighting factor was applied when the trajectory points were less than twice this average, as suggested by Zeng and Hopke [39].

$$W_{ij} = \begin{cases} 1.0, & n_{ij} > 2 \cdot n_{ave} \\ 0.75, & n_{ave} < n_{ij} \leq 2 \cdot n_{ave} \\ 0.5, & 0.5 \cdot n_{ave} < n_{ij} \leq n_{ave} \\ 0.15, & n_{ij} < 0.5 \cdot n_{ave} \end{cases} \quad (4)$$

2.5. CWT Model

The PSCF model determines backward trajectories that display concentrations exceeding specific thresholds (in this study, the 24 h environmental standard of $50 \mu\text{g m}^{-3}$). However, this approach has an inherent drawback: it might underestimate trajectories with even greater concentrations, making it challenging to differentiate and assess them individually. The CWT model combines the back trajectory with the concentration in the measurement area to express the degree of impact of the back trajectory through each grid cell on the measurement area as a concentration (Equation (5)) [40]. The weighting factor is applied identically, as in the case of PSCF.

$$CWT_{ij} = \left(\frac{1}{\sum_{T=1}^M \tau_{ijT}} \right) \times \sum_{T=1}^M C_{\tau_{ijT}} \quad (5)$$

where CWT_{ij} represents the 1 h $\text{PM}_{2.5}$ concentration within grid cell ij at the time the backward trajectory arrives, C is the concentration observed on arrival of trajectory T , τ_{ijT} is the number of trajectory segment endpoints for an individual backward trajectory (T) as it passes through a $0.5^\circ \times 0.5^\circ$ grid cell ij , i is the index of the trajectory, and M is the total number of back trajectories.

3. Results

3.1. Temporal Variation of $\text{PM}_{2.5}$

During the analysis period in Porto Velho, the average $\text{PM}_{2.5}$ concentration was $17.7 \pm 24.0 \mu\text{g m}^{-3}$, equivalent to Brazil's annual standard of $17 \mu\text{g m}^{-3}$. Wildfires contribute more than 80% of $\text{PM}_{2.5}$ during the dry season in the western Amazon region [41]. During the wildfire season, July through October, the average concentration was $34.2 \mu\text{g m}^{-3}$, seven times higher than the average for the wet season (December–May), with more than 25% of high concentrations above $100 \mu\text{g m}^{-3}$ occurring in August when the average concentration was $54.5 \mu\text{g m}^{-3}$ (Figure 1).

In the Amazon basin, including Porto Velho, observational studies on $\text{PM}_{2.5}$ are scarce, with the majority of the research being dated (Table 1). The most commonly employed method is filter-based, and for low-cost sensors (LCS), a laser light source is utilized to measure $\text{PM}_{2.5}$. In Mauna, located in the Amazonas state, and in Porto Velho of the Rondônia state, samples were collected using filters over durations of two to five days. In Iranduba, also in the Amazonas state, sampling on the filters lasted for 10 h. Conversely, in the Rio Blanco area of the Acre state, real-time measurements were conducted utilizing low-cost sensors with a laser light source, and the analyzed data were based on daily averages. However, these studies yielded low-resolution data, presenting challenges in accurately capturing daily variations in ambient conditions.

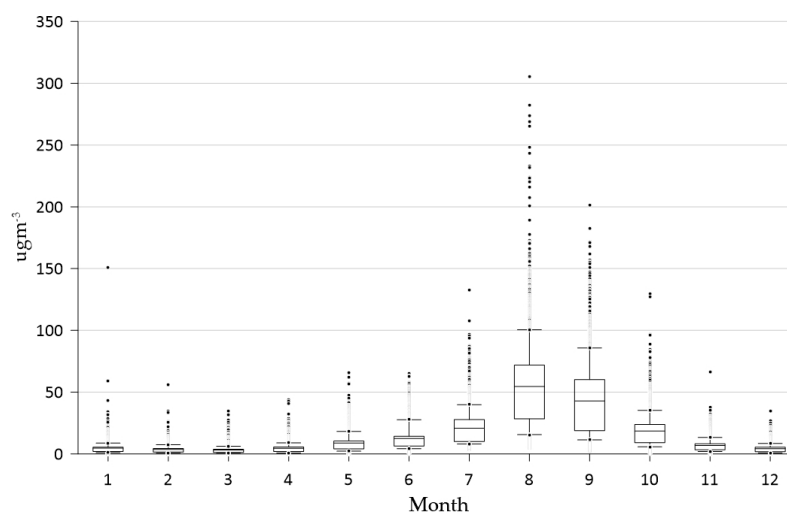


Figure 1. Box plot of the monthly concentration of $PM_{2.5}$ from April 2020 to October 2022 in Porto Velho. The horizontal line in a box is the mean value. The lower and upper whiskers represent 10% and 90%, respectively.

Table 1. Comparison of $PM_{2.5}$ average concentrations with those of previous studies in the Amazon rainforest, Brazil.

Location (State)	Year	$PM_{2.5}$ ($\mu\text{g m}^{-3}$)	Reference
Manaus (Amazonas)	2008–2012	2.4 (January–June 1.3, July–December 3.4)	Artaxo et al. [42]
Porto Velho (Rondonia)	2009–2012	21.6 (January–June 10.2, July–December 33.0)	Artaxo et al. [42]
Irlanduba (Amazonas)	2016	4.7 March–April 6.7 August–September	Fernandes et al. [43]
Rio Branco (Acre state)	2018–2019	10.1	Coker et al. [31]
Porto Velho (Rondonia)	2020–2022	17.7 (January–June 6.2 July–December 24.6)	This study

In the state of Amazonas, both the Irlanduba and Mauna regions maintained notably clean air quality in terms of $PM_{2.5}$ concentrations. Emissions in the Irlanduba area originated from fugitive dust, open burning, and vehicles, while the Mauna region was influenced by long-range pollutants from forest fires. In Porto Velho, the average $PM_{2.5}$ concentration measured from 2008 to 2012 was 28.6% higher than in this study due to a drought in 2010 that increased wildfires.

In the region of Porto Velho, diurnal variations of $PM_{2.5}$ exhibited distinct characteristics between the rainy (December–May) season and periods of wildfire (Figure 2). During the rainy season, the peak concentration occurred at 20:00 Local Time (LT), while the minimum concentration was observed at 6:00 LT. In contrast, during wildfire periods, concentrations were generally lower during the day, but from dawn until 7:00 LT, the $PM_{2.5}$ concentration surged to its daily maximum. The diurnal variation of $PM_{2.5}$ during wildfire periods correlated with the diurnal attributes of wind speed and mixing height. As the wind speed increased and the mixing height rose during the day, $PM_{2.5}$ concentrations decreased due to enhanced dispersion and dilution. However, starting from 18:00 LT, when the mixing height reduced and the wind speed weakened, there was a rising trend in $PM_{2.5}$ concentrations. By 20:00 LT, with the mixing height dropping to 70 m, $PM_{2.5}$ concentrations

intensified, continuing this upward trend until 7:00 LT the next morning. This can be attributed to the weaker horizontal dispersion and the challenges in dilution at night when the mixing height is exceptionally low, especially during wildfires. When high concentrations of $PM_{2.5}$ are introduced indoors during the nighttime, the duration of their presence indoors increases, leading to elevated levels of $PM_{2.5}$ concentration within the indoor environment [43]. During the day, if smoke plumes from wildfires enter the atmosphere and stagnate by evening, the resulting decrease in mixing height and concentration can adversely impact the air quality in Porto Velho. The average $PM_{2.5}$ concentrations during the rainy season and wildfire periods were 4.8 ± 5.8 and $34.2 \pm 30.1 \mu\text{g m}^{-3}$, respectively. This underscores the fact that although rising mixing heights can lead to decreased $PM_{2.5}$ concentrations, increased wildfires can boost both the peak and minimum concentrations in the diurnal pattern. In August, the average wind speed reduced by 67% compared to that in the rainy season, while the maximum and minimum wind speeds decreased by 63% and 48.5%, respectively. This reduction in wind speed, leading to minimal horizontal dispersion, contributed to the elevated $PM_{2.5}$ concentrations. Additionally, the relative humidity in Porto Velho was, on average, 27.2% lower at 16:00 LT during wildfire periods compared to during the rainy season, providing more favorable conditions for wildfire occurrences.

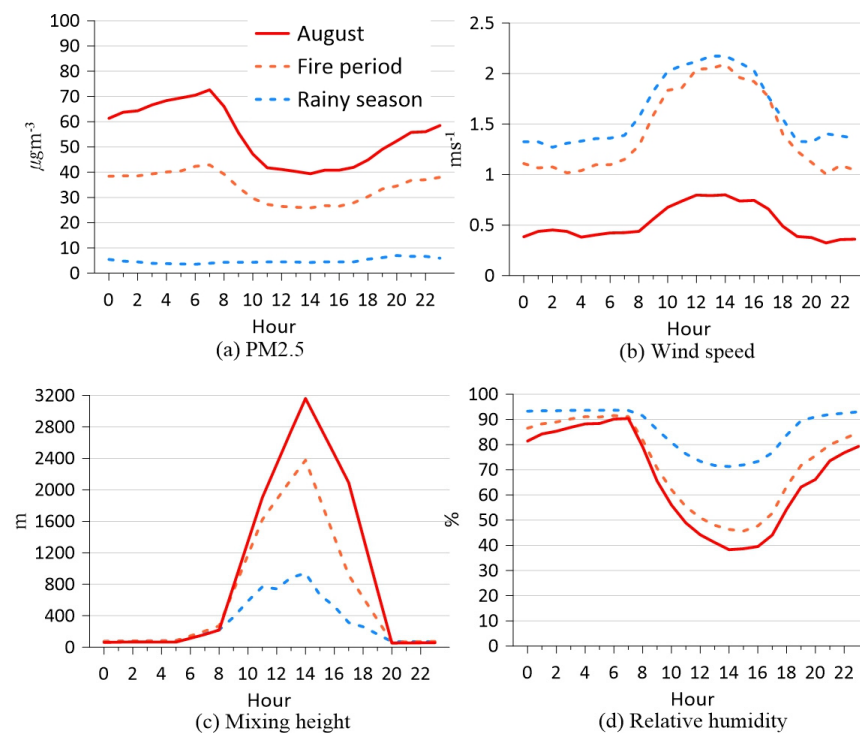


Figure 2. Diurnal variation of $PM_{2.5}$, wind speed, mixing height, and relative humidity at Porto Velho.

3.2. $PM_{2.5}$ Concentrations Based on Wildfire Occurrence and Wind Conditions

Figure 3a shows the average annual number of wildfires within 30 km of the study area and the number of wildfires during the fire season from July to October. From 2012 to 2022, there was an average of 1121 wildfires per year, and trends in wildfire occurrence were not statistically significant (Theil-Sen, $p > 0.05$). Most wildfires occurred during the July to October fire season, accounting for 92.9% of annual wildfires. In particular, an average of 15.7 wildfires per day occurred in August, when 42% of the annual wildfires occurred.

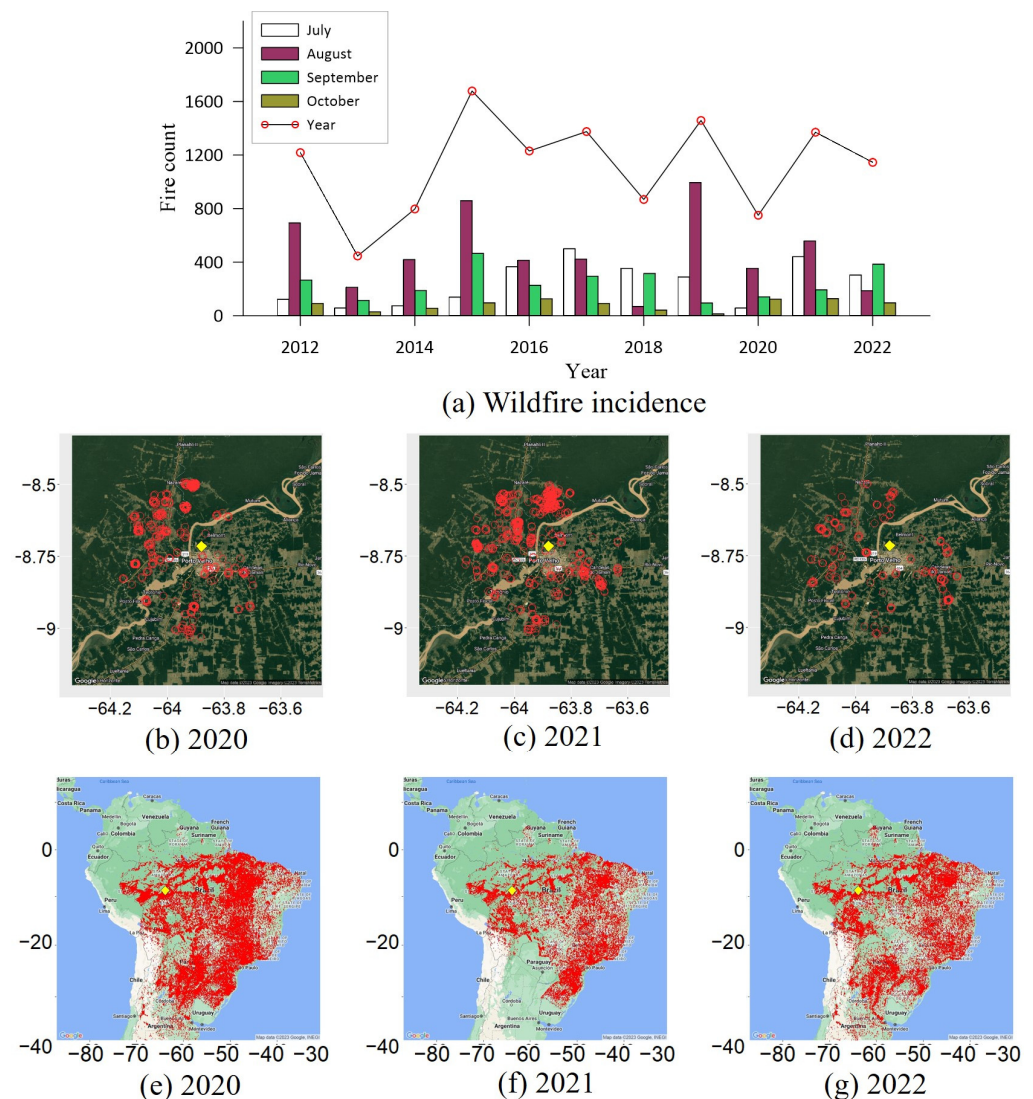


Figure 3. Wildfires near the station and in the Amazon rainforest. (a) Wildfires within 30 km of the station (2012 to 2022). (b–d) Wildfires occurred in August within 30 km of stations (2020–2022). (e–g) August wildfires in Brazil, Bolivia, and Paraguay (2020–2022). The yellow diamonds indicate the PM_{2.5} measurement locations.

Figure 3b shows the wildfires that occurred within 30 km of the measurement site during the analysis period in August when PM_{2.5} concentrations were the highest. Figure 3c shows the wildfires that occurred during the analysis period in August in Brazil. During a wildfire season, plumes from wildfires in upwind areas can also contribute to PM_{2.5} enhancement and those near the measurement site [44]. Higher mixing heights can increase the vertical rise of wildfire plumes, which can increase PM_{2.5} concentrations in the atmosphere in the downwind region [45].

Wildfires that frequently occur within a 30 km radius of the measurement station can impact the PM_{2.5} concentration levels at the station, contingent on the wind direction and speed. During the period of wildfire occurrences, the wind direction in the Porto Velho region was most frequently northerly and southerly, accounting for 28.4% and 16.4% of the time, respectively (Figure 4). In westerly, southwesterly, and northwesterly winds, light winds of 0–2 ms^{−1} occurred at an average rate of 95.5%, while relatively strong winds exceeding 4 ms^{−1} were infrequent, averaging just 0.2%. In contrast, easterly, southeasterly, and northeasterly winds had a comparatively higher percentage of winds exceeding 4 ms^{−1}, averaging 9.2%, while light winds made up an average of 67.4%.

Northerly and southerly winds predominantly had light winds of $0\text{--}2\text{ ms}^{-1}$, occurring 77.5% and 78.7% of the time, respectively, with relatively strong winds of 4 m/s or more occurring 2.5% and 6.1% of the time.

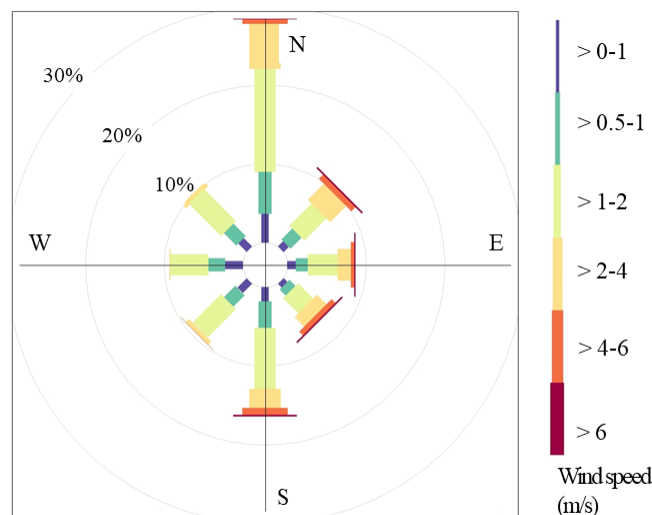


Figure 4. Wind rose during the wildfire period in Porto Velho.

As for the $\text{PM}_{2.5}$ concentration according to wind direction, westerly, northwesterly, northerly, and southwesterly winds exhibited concentrations of $36.8 \pm 30.2\ \mu\text{g m}^{-3}$, $35.6 \pm 25.2\ \mu\text{g m}^{-3}$, $32.8 \pm 27.8\ \mu\text{g m}^{-3}$, and $32.7 \pm 28.3\ \mu\text{g m}^{-3}$, respectively. Conversely, the concentrations of $\text{PM}_{2.5}$ in southeasterly, southerly, easterly, and northeasterly winds were distributed at $26.4 \pm 25.6\ \mu\text{g m}^{-3}$, $27.5 \pm 26.1\ \mu\text{g m}^{-3}$, $27.5 \pm 25.3\ \mu\text{g m}^{-3}$, and $30.1 \pm 25.2\ \mu\text{g m}^{-3}$, respectively.

3.3. SDG Indicator 11.6.2 and Air Quality Index (AQI)

Good air quality is vital for the sustainable well-being of citizens. The Sustainable Development Goal (SDG) Indicator 11.6.2 quantifies the “annual mean levels of fine particulate matter (e.g., $\text{PM}_{2.5}$) in cities (population-weighted)”. In Brazil, the annual standard for $\text{PM}_{2.5}$ is set at $17\ \mu\text{g m}^{-3}$. For 2021, the Porto Velho region recorded an annual average $\text{PM}_{2.5}$ concentration of $16.9 \pm 25.3\ \mu\text{g m}^{-3}$, meeting the annual environmental standard. Nevertheless, this value is three times higher than the World Health Organization (WHO)’s annual guideline of $5\ \mu\text{g m}^{-3}$.

During the rainy season, the $\text{PM}_{2.5}$ concentration fully met Brazil’s standard and achieved 96.7% of the WHO’s standard (24 h environmental standard at $15\ \mu\text{g m}^{-3}$). However, during the wildfire season, these concentrations met 78.3% of Brazil’s standard and only 23% of the WHO’s standard. Specifically, in August, the concentrations complied with 48.9% of Brazil’s standard and a mere 8.7% of the WHO’s criteria.

The Brazilian government has established a five-tier air quality index to help citizens understand and respond to health risks associated with air quality conditions. The AQI for $\text{PM}_{2.5}$ consistently indicated a “Good” index during the rainy season. During the wildfire period, there was a 21.2% occurrence above the “Bad” index, and this proportion increased to 51.1% in August (Table 2). When the AQI deteriorated from a “Good” index to a “Hazardous” index, the wind speed decreased by 0.4 ms^{-1} and 0.3 ms^{-1} during the wildfire period and in August, respectively. The average wind speed of 0.7 ms^{-1} in August corresponds to the daytime (from 12:00 to 18:00 LT) average seen in Figure 2b, while 0.4 ms^{-1} is on par with the average wind speed at night (from 17:00 to 06:00), illustrating the difference in wind speeds between daytime and nighttime. The lower average wind speeds in wildfire period and August when the AQI index is categorized as “Very Bad” and “Hazardous” suggest a low mixing height and stagnant air conditions, predominantly

during nighttime. Visibility, which provides a direct visual indication of air quality status for citizens, deteriorated by 77.1% during the wildfire period and by 75% in August.

Table 2. Wildfire frequency, visibility, and wind speed characteristics by AQI, Brazil.

AQI	Range of PM _{2.5} Concentration (24 h Average, $\mu\text{g m}^{-3}$)	July–October			August		
		Frequency (%)	Visibility (km)	Wind Speed (ms^{-1})	Frequency (%)	Visibility (km)	Wind Speed (ms^{-1})
Good	0–25	49.7	22.7	1.5	16.3	22.6	0.7
Moderate	>25–50	29.1	21.1	1.5	32.6	20.3	0.6
Bad	>50–75	13.3	14.2	1.4	31.5	12.8	0.5
Very Bad	>75–125	7.0	8.9	1.1	17.4	8.8	0.5
Hazardous	>125	0.9	5.2	1.1	2.2	5.6	0.4

3.4. Estimation of PM_{2.5} Sources

3.4.1. Conditional Probability Function (CPF) and Polar Annulus

CPF analysis serves as a valuable method for assessing the sources of specific PM_{2.5} concentrations, taking into account wind speed and direction. The AQI uses a 24 h average, which exhibited a maximum wind speed difference of 0.4 m/s during wildfire periods. However, CPF analysis employs hourly data, thus revealing a significant fluctuation in wind speeds, ranging from a minimum of 0.1 ms^{-1} to a maximum of 13 ms^{-1} (Figure 5). When the hourly PM_{2.5} concentration was measured at 14 $\mu\text{g m}^{-3}$ or lower, the predominant winds were either southeasterly, ranging from 8 to 14 ms^{-1} , or easterly winds of 4 ms^{-1} or higher (Figure 5a). For PM_{2.5} concentrations between 15 and 25 $\mu\text{g m}^{-3}$, northwesterly winds exceeding 4 ms^{-1} were the main contributing factor (Figure 5b).

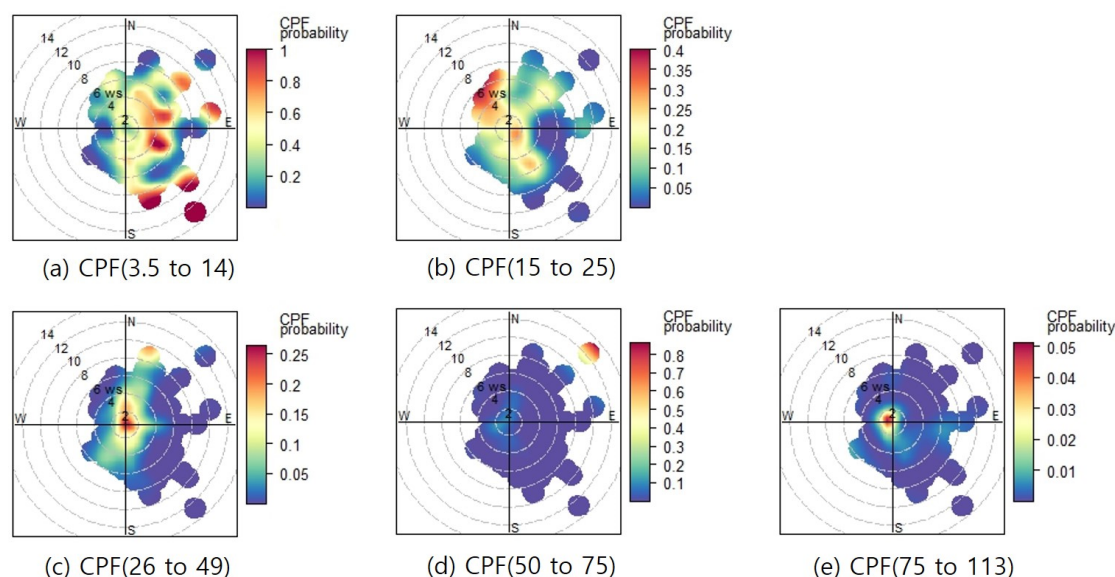


Figure 5. Results of conditional probability function based on PM_{2.5} ($\mu\text{g m}^{-3}$) concentration distribution. High CPF values are indicated in red, while low values are shown in blue.

At moderate air quality levels, where PM_{2.5} concentrations were between 25 and 50 $\mu\text{g m}^{-3}$, weaker winds of 2 ms^{-1} or less were influential (Figure 5c). However, at poor air quality levels with PM_{2.5} concentrations ranging from 50 to 75 $\mu\text{g m}^{-3}$, strong northeasterly winds between 12 and 14 ms^{-1} were prevalent (Figure 5d). Moreover, in instances where PM_{2.5} concentrations exceeded 75 $\mu\text{g m}^{-3}$ (Figure 5e), the distribution occurred under conditions of low wind speed and stagnant air.

The CPF analysis demonstrated that the distribution of PM_{2.5} concentrations varies based on the characteristics of wind direction and speed. The polar annulus approach is

used to analyze how $PM_{2.5}$ concentrations change over time based on the wind direction (Figure 6). In the Porto Velho region, higher concentrations of $PM_{2.5}$ were observed from nighttime to morning in the northerly wind sector and from dawn to daytime over an extended period in the westerly wind sector (Figure 6a). In the easterly wind, high concentrations of $PM_{2.5}$ were distributed from late dawn to morning. In the Porto Velho region, daytime $PM_{2.5}$ concentrations are comparatively lower, largely driven by the strong easterly wind influx. Conversely, the elevated $PM_{2.5}$ concentrations observed in the westerly wind patterns can be attributed to the prevailing weaker wind velocities (Figure 6b). Visibility is a good indicator of air quality, including pollutants such as $PM_{2.5}$ [46]. In this region, the visibility was excellent when the southeasterly wind system, which has high wind speed and low $PM_{2.5}$ concentration, was introduced (Figure 6c). Furthermore, atmospheric pressure was observed to be relatively higher in the southerly wind and lower with northerly and westerly winds (Figure 6d). Such observations imply that wildfires may occur more frequently in the north and west than in the southern regions.

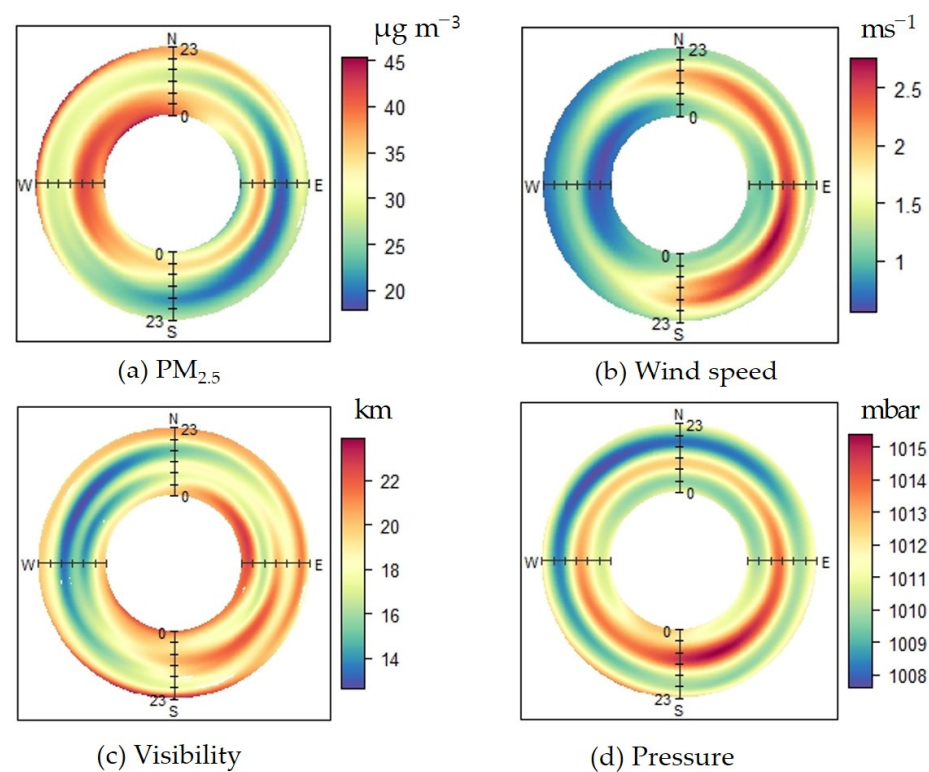


Figure 6. The polar annulus plot analysis for Porto Velho visualizing the $PM_{2.5}$ concentration, wind speed, visibility, and pressure in relation to wind direction using color mapping.

3.4.2. Back Trajectory Analysis

In the Amazon rainforest, $PM_{2.5}$ from forest fires can affect hundreds of kilometers of horizontal distances [11]. Moreover, plumes of wildfire smoke can rise as high as 2500 m and, depending on weather conditions, influence $PM_{2.5}$ enhancement in downwind areas [47]. Back trajectory analysis can assess the contribution of $PM_{2.5}$ from wildfires to the target area through horizontal and vertical transport [44,48].

Figure 7a displays the probability of trajectories with $PM_{2.5}$ concentrations exceeding $50 \mu g m^{-3}$ crossing each grid. This suggests pollution sources in the North Region (comprising the states of Amazonas and Pará). The CWT analysis further indicated that areas contributing to the $PM_{2.5}$ in Porto Velho include parts of the North and Central-West regions (the states of Mato Grosso, Figure 7b). From 2020 to 2022, in Mato Grosso, Para, and Amazonas, the areas damaged by wildfires constituted 42.9% (471,721 ha), 0.7%, and 0.09%, respectively, of the total wildfire-affected areas in Brazil [49].

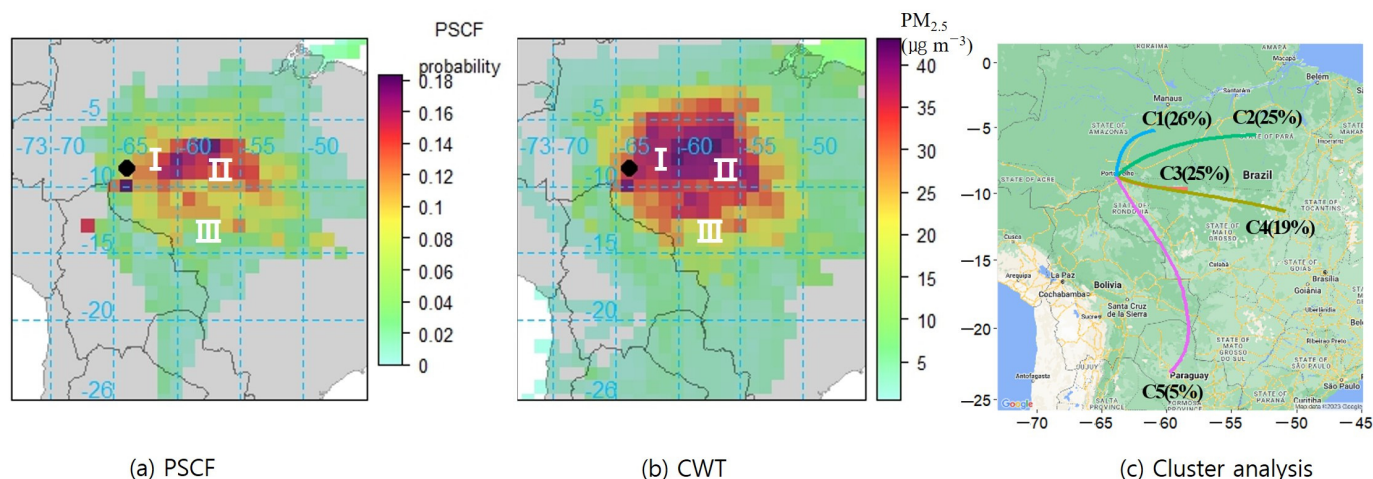


Figure 7. Trajectory source contribution with PSCF, CWT, and cluster analyses (Black circle: Porto Velho, I: state of Amazonas, II: state of Pará, III: state of Mato Grosso).

Figure 7c shows the five clusters of winds entering the station, with the influence of northeasterly winds (Clusters 1 and 2), southeasterly winds (Clusters 3 and 4), and southerly winds (Cluster 5). $PM_{2.5}$ concentrations from Clusters 2, 3, and 4 were 38.6 , 34.6 , and $37.6 \mu g m^{-3}$. Cluster 1 was $28.4 \mu g m^{-3}$, and Cluster 5 was $24.3 \mu g m^{-3}$. Cluster 5 reflected the longest pathway from Paraguay and Bolivia. Clusters 2 and 4 had relatively fast inflows from Para and Mato Gosso. Clusters 1 and 3 had shorter travel paths, reflecting the impact of wildfires in areas close to Porto Velho. Deforestation is a major cause of wildfires in the Brazilian Amazon region, and deforestation occurs along roads. Cluster 1 and Cluster 2 were found to be affected by wildfires occurring in the area around highways 319 and 230 [50–52]; therefore, policies to reduce wildfires are needed to reduce exposure to high concentrations of $PM_{2.5}$ for citizens along roads and in downwind areas [48,53]. Cluster 2, Cluster 4, and Cluster 5 traveled relatively long distances through wildfire areas, contributing to the deterioration of air quality in the region. This is because the more wildfires that occur, the more likely air traveling through the wildfire zone will contain high concentrations of $PM_{2.5}$ [54].

4. Discussion

The Porto Velho region is known for its recurrent forest fires due to deforestation. Nevertheless, with a population of approximately 500,000, research on their $PM_{2.5}$ exposure has been notably limited. In particular, there has been no detailed study on the hourly distribution of $PM_{2.5}$ and the areas most affected by forest fires regarding air quality.

The $PM_{2.5}$ concentration in the Porto Velho region was consistent with Brazil's annual environmental standards. However, from July to October, the period recognized as the wildfire period, there was a notable increase in $PM_{2.5}$ concentrations attributed to the rise in wildfires, wind velocities, and mixing height.

During wildfire periods, $PM_{2.5}$ concentrations increased from 20:00 to 07:00 LT, corresponding to mixing height and wind speed changes. While decreased mixing height intensified $PM_{2.5}$ concentrations, the continued rise until 07:00 LT indicates wildfires as a significant $PM_{2.5}$ source during the night and early morning. Wildfires during these hours further enhance $PM_{2.5}$ concentrations due to limited vertical dispersion [55,56].

During the day, increased wildfire activity can elevate $PM_{2.5}$ concentrations [57,58]. This can intensify $PM_{2.5}$ concentrations in downwind areas, especially in the afternoon when wind speed drops and mixing height decreases [58,59]. These patterns are pronounced in diurnal variations, particularly during wildfire seasons and in August. Despite the increased mixing height in August, the $PM_{2.5}$ concentrations peaked due to frequent wildfires and a 67% decrease in wind speed compared to those of the rainy season, hindering $PM_{2.5}$ dispersion.

In Porto Velho, PM_{2.5} concentrations during wildfire seasons need reduction to meet SDG Indicator 11.6.2. The air quality index indicated “Bad” or worse levels in 21.2% of the period, with August reaching a concerning 51.1%. This poses significant health risks to its inhabitants.

In the Porto Velho region, northerly and westerly winds correlated with increased PM_{2.5} concentrations due to frequent wildfires. In contrast, stronger southerly or easterly winds led to decreased PM_{2.5} concentrations and clearer visibility, with the highest levels observed in the early to mid-morning. The main long-distance pollution contributors were wildfires from Amazonas, Para, and Mato Grosso. Cluster analysis also highlighted air influx from northeastern highways, central areas, and regions in Paraguay and Bolivia.

In the Amazon rainforest region, including the Porto Velho area, the absence of regulatory-grade monitoring stations precludes direct comparison with PurpleAir’s measurement data. However, the PM_{2.5} emitted from the wildfires in the Amazon can settle in areas where residents of downwind regions live [47]. Low-cost sensors allow for real-time data collection from multiple monitoring points, enabling the construction of diverse datasets. Through this, the accuracy of the analysis can be enhanced [33]. Consequently, evaluating emission source characteristics through even low-cost sensors is an essential preliminary study to formulate policies to reduce PM_{2.5}.

Local wildfires from the north and west, along with long-range transport from wildfires from Mato Grosso, Amazonas, and Para, impact PM_{2.5} concentrations in the region. To achieve clean air goals (SDG Indicator 11.6.2), mitigating these wildfires and reducing deforestation in Brazil’s northern and central areas is crucial. Given the immediate and long-term impacts of elevated PM_{2.5} levels, the results of this study underscore the urgent need for comprehensive policies aimed at improving air quality.

Author Contributions: Y.-W.J.: conceptualization, formal analysis, visualization, investigation, writing; G.-W.J.: conceptualization, writing—review and editing, supervision. All authors have read and agreed to the published version of the manuscript.

Funding: This work was supported by a grant from the Ministry of Education and the National Research Foundation of Korea (NRF-2019S1A6A3A02058027). And this work was also supported by the Hankuk University of Foreign Studies Research Fund of 2023.

Institutional Review Board Statement: Not applicable.

Informed Consent Statement: Not applicable.

Data Availability Statement: The datasets analyzed during the current study are available in the PurpleAir repository, accessible via <https://www.purpleair.com/> (accessed on 30 July 2023). To download the related materials, you can install and use the PurpleAir Download Tool, available at <https://community.purpleair.com/t/purpleair-data-download-tool/3787> (accessed on 30 July 2023).

Acknowledgments: The authors are grateful to the Ministry of Education of the Republic of Korea and Hankuk University of Foreign Studies for their support.

Conflicts of Interest: These authors declare no conflict of interest.

References

1. Emmanoella, C.G.A.; Carlos, R.S.; Ana, P.D.C.; Allan, L.P.; Gabriel, A.O.; Thiago, C.S. Global review and state-of-the-art of biomass and carbon stock in the Amazon. *J. Environ. Manag.* **2023**, *331*, 117251. [CrossRef]
2. Phillips, O.L.; Brienen, R.J.W.; The RAINFOR Collaboration. Carbon uptake by mature Amazon forests has mitigated Amazon nations’ carbon emissions. *Carbon. Balance Manag.* **2017**, *12*, 1. [CrossRef]
3. Pereira, A.S.A.; Santos, V.J.; Alves, S.; Amaral e Silva, A.; Silva, C.G.; Calijuri, M.L. Contribution of rural settlements to the deforestation dynamics in the Legal Amazon. *Land. Use Policy* **2022**, *115*, 106039. [CrossRef]
4. Olson, N.; Boaggio, K.; Rice, B.; Foley, K.; LeDuc, S. Wildfires in the western United States are mobilizing PM_{2.5}-associated nutrients and may contribute to downwind cyanobacteria blooms. *Environ. Sci. Process Impacts* **2023**, *25*, 1049–1066. [CrossRef] [PubMed]
5. Basso, L.S.; Wilson, C.; Chipperfield, M.P.; Tejada, G.; Cassol, H.L.G.; Arai, E.; Williams, M.; Smallman, T.L.; Peters, W.; Naus, S.; et al. Atmospheric CO₂ inversion reveals the Amazon as a minor carbon source caused by fire emissions, with forest uptake offsetting about half of these emissions. *Atmos. Chem. Phys.* **2023**, *23*, 9658–9723. [CrossRef]

6. Gatti, L.V.; Basso, L.S.; Miller, J.B.; Gloor, M.; Gatti Domingues, L.; Cassol, H.L.G.; Tejada, G.; Aragão, L.E.O.C.; Nobre, C.; Peters, W.; et al. Amazonia as a carbon source linked to deforestation and climate change. *Nature* **2021**, *595*, 388–393. [[CrossRef](#)]
7. Wilmot, T.Y.; Mallia, D.V.; Hallar, A.G.; Lin, J.C. Wildfire plumes in the Western US are reaching greater heights and injecting more aerosols aloft as wildfire activity intensifies. *Sci. Rep.* **2022**, *12*, 12400. [[CrossRef](#)]
8. Yuan, S.; Bao, F.; Zhang, X.; Li, Y. Severe Biomass-Burning Aerosol Pollution during the 2019 Amazon Wildfire and Its Direct Radiative-Forcing Impact: A Space Perspective from MODIS Retrievals. *Remote Sens.* **2022**, *14*, 2080. [[CrossRef](#)]
9. Kramer, A.L.; Liu, J.; Li, L.; Connolly, R.; Barbato, M.; Zhu, Y. Environmental justice analysis of wildfire-related PM_{2.5} exposure using low-cost sensors in California. *Sci. Total Environ.* **2023**, *15*, 159218. [[CrossRef](#)] [[PubMed](#)]
10. Ma, Y.; Zang, E.; Liu, Y.; Lu, Y.; Krumholz, H.M.; Bell, M.L.; Chen, K. Wildfire smoke PM_{2.5} and mortality in the contiguous United States. *medRxiv* **2023**. [[CrossRef](#)]
11. Prist, P.R.; Sangermano, F.; Bailey, A.; Bugni, V.; Villalobos-Segura, M.C.; Pimiento-Quiroga, N.; Daszak, P.; Zambrana-Torrel, C. Protecting Brazilian Amazon Indigenous territories reduces atmospheric particulates and avoids associated health impacts and costs. *Commun. Earth Environ.* **2023**, *4*, 34. [[CrossRef](#)]
12. Aguilera, R.; Corringham, T.; Gershunov, A.; Benmarhnia, T. Wildfire smoke impacts respiratory health more than fine particles from other sources: Observational evidence from Southern California. *Nat. Commun.* **2021**, *12*, 1493. [[CrossRef](#)] [[PubMed](#)]
13. Childs, M.L.; Li, J.; Wen, J.; Heft-Neal, S.; Driscoll, A.; Wang, S.; Gould, C.F.; Qiu, M.; Burney, J.; Burke, M. Daily Local-Level Estimates of Ambient Wildfire Smoke PM_{2.5} for the Contiguous US. *Environ. Sci. Technol.* **2022**, *56*, 13607–13621. [[CrossRef](#)] [[PubMed](#)]
14. Cleland, S.E.; Wyatt, L.H.; Wei, L.; Paul, N.; Serre, M.L.; West, J.J.; Henderson, S.B.; Rappold, A.G. Short-Term Exposure to Wildfire Smoke and PM_{2.5} and Cognitive Performance in a Brain-Training Game: A Longitudinal Study of U.S. Adults. *Environ. Health Perspect.* **2022**, *130*, 67005. [[CrossRef](#)] [[PubMed](#)]
15. Yu, P.; Xu, R.; Li, S.; Yue, X.; Chen, G.; Ye, T.; Coêlho, M.S.Z.S.; Saldiva, P.H.N.; Sim, M.R.; Abramson, M.J.; et al. Exposure to wildfire-related PM_{2.5} and site-specific cancer mortality in Brazil from 2010 to 2016: A retrospective study. *PLoS Med.* **2022**, *19*, e1004103. [[CrossRef](#)]
16. Zhou, X.; Josey, K.; Kamareddine, L.; Caine, M.C.; Liu, T.; Mickley, L.J.; Cooper, M.; Dominici, F. Excess of COVID-19 cases and deaths due to fine particulate matter exposure during the 2020 wildfires in the United States. *Sci. Adv.* **2021**, *13*, eabi8789. [[CrossRef](#)]
17. Dong, J.; Wang, Y.; Wang, L.; Zhao, W.; Huang, C. Assessment of PM_{2.5} exposure risk towards SDG indicator 11.6.2—A case study in Beijing. *Sustain. Cities Soc.* **2022**, *82*, 103864. [[CrossRef](#)]
18. Yin, Z.; Zhang, L.; Roradeh, H.; Baaghideh, M.; Yang, Z.; Hu, K.; Liu, L.; Zhang, Y.; Mayvaneh, F.; Zhang, Y. Reduction in daily ambient PM_{2.5} pollution and potential life gain by attaining WHO air quality guidelines in Tehran. *Environ. Res.* **2022**, *209*, 112787. [[CrossRef](#)]
19. Chen, G.; Guo, Y.; Yue, X.; Tong, S.; Gasparrini, A.; Bell, M.L.; Armstrong, B.; Schwartz, J.; Jaakkola, J.J.K.; Zanobetti, A.; et al. Mortality risk attributable to wildfire-related PM_{2.5} pollution: A global time series study in 749 locations. *Lancet Planet. Health* **2021**, *5*, e579–e587. [[CrossRef](#)]
20. Ye, T.; Xu, R.; Yue, X.; Chen, G.; Yu, P.; Coelho, M.; Paulo, H.; Abramson, M.; Guo, Y.; Li, S. Short-term exposure to wildfire-related PM_{2.5} increases mortality risks and burdens in Brazil. *Nat. Commun.* **2022**, *13*, 7651. [[CrossRef](#)]
21. Apte, J.; Brauer, M.; Cohen, A.; Ezzati, M.; Pope, C. Ambient PM_{2.5} Reduces Global and Regional Life Expectancy. *Environ. Sci. Technol. Lett.* **2018**, *5*, 546–551. [[CrossRef](#)]
22. Tsai, S.S.; Chen, C.C.; Yang, C.Y. The impacts of reduction in ambient fine particulate (PM_{2.5}) air pollution on life expectancy in Taiwan. *J. Toxicol. Environ. Health A* **2022**, *17*, 913–920. [[CrossRef](#)] [[PubMed](#)]
23. Ardon-Dryer, K.; Dryer, Y.; Williams, J.N.; Moghimi, N. Measurements of PM_{2.5} with PurpleAir under atmospheric conditions. *Atmos. Meas. Tech.* **2020**, *13*, 5441–5458. [[CrossRef](#)]
24. Brito, J.; Rizzo, L.V.; Morgan, W.T.; Coe, H.; Johnson, B.; Haywood, J.; Longo, K.; Freitas, S.; Andreae, M.O.; Artaxo, P. Ground-based aerosol characterization during the South American Biomass Burning Analysis (SAMBBA) field experiment. *Atmos. Chem. Phys. Discuss.* **2013**, *14*, 11002. [[CrossRef](#)]
25. Butt, E.W.; Conibear, L.; Knote, C.; Spracklen, D.V. Large Air Quality and Public Health Impacts due to Amazonian Deforestation Fires in 2019. *Geohealth* **2021**, *5*, e2021GH000429. [[CrossRef](#)]
26. Sørensen, M.; Daneshvar, B.; Hansen, M.; Dragsted, L.O.; Hertel, O.; Knudsen, L.; Loft, S. Personal PM_{2.5} exposure and markers of oxidative stress in blood. *Environ. Health Perspect.* **2003**, *111*, 161–166. [[CrossRef](#)]
27. Urrutia-Pereira, M.; Rizzo, L.V.; Chong-Neto, H.J.; Solé, D. Impact of exposure to smoke from biomass burning in the Amazon rain forest on human health. *J. Bras. Pneumol.* **2021**, *15*, e20210219. [[CrossRef](#)]
28. Preisler, H.K.; Schweizer, D.; Cisneros, R.; Procter, T.; Ruminski, M.; Tarnay, L. A statistical model for determining impact of wildland fires on Particulate Matter (PM_{2.5}) in Central California aided by satellite imagery of smoke. *Environ. Pollut.* **2015**, *205*, 340–349. [[CrossRef](#)]
29. Zhang, H.; Kondragunta, S. Daily and Hourly Surface PM_{2.5} Estimation from Satellite AOD. *Earth Space Sci.* **2021**, *8*, e2020EA001599. [[CrossRef](#)]
30. Barkjohn, K.K.; Gantt, B.; Clements, A.L. Development and Application of a United States wide correction for PM_{2.5} data collected with the PurpleAir sensor. *Atmos. Meas. Tech.* **2021**, *22*, 4617–4637. [[CrossRef](#)]

31. Coker, E.S.; Buralli, R.; Manrique, A.F.; Kanai, C.M.; Amegah, A.K.; Gouveia, N. Association between PM_{2.5} and respiratory hospitalization in Rio Branco, Brazil: Demonstrating the potential of low-cost air quality sensor for epidemiologic research. *Environ. Res.* **2022**, *214*, 113738. [[CrossRef](#)] [[PubMed](#)]
32. Raheja, G.; Sabi, K.; Sonla, H.; Gbedjangni, E.K.; McFarlane, C.M.; Hodoli, C.G.; Westervelt, D.M. A network of field-calibrated low-cost sensor measurements of PM_{2.5} in Lomé, Togo, over one to two years. *ACS Earth Space Chem.* **2022**, *6*, 1011–1021. [[CrossRef](#)] [[PubMed](#)]
33. Barkjohn, K.K.; Holder, A.L.; Frederick, S.G.; Clements, A.L. Correction and Accuracy of PurpleAir PM_{2.5} Measurements for Extreme Wildfire Smoke. *Sensors* **2022**, *22*, 9669. [[CrossRef](#)] [[PubMed](#)]
34. Caseiro, A.; Schmitz, S.; Villena, G.; Jagatha, J.V.; von Schneidmesser, E. Ambient characterisation of PurpleAir particulate matter monitors for measurements to be considered as indicative. *Environ. Sci. Atmos.* **2022**, *2*, 1400–1410. [[CrossRef](#)]
35. Heintzelman, A.; Filippelli, G.M.; Moreno-Madriñan, M.J.; Wilson, J.S.; Wang, L.; Druschel, G.K.; Lulla, V.O. Efficacy of Low-Cost Sensor Networks at Detecting Fine-Scale Variations in Particulate Matter in Urban Environments. *Int. J. Environ. Res. Public Health.* **2023**, *20*, 1934. [[CrossRef](#)]
36. Urbanski, S.; Nordgren, B.; Albury, C.; Schwert, B.; Peterson, D.; Quayle, B.; Hao, W. A VIIRS direct broadcast algorithm for rapid response mapping of wildfire burned area in the western United States. *Remote Sens. Environ.* **2018**, *219*, 271–283. [[CrossRef](#)]
37. Vadrevu, K.; Lasko, K. Intercomparison of MODIS AQUA and VIIRS I-Band Fires and Emissions in an Agricultural Landscape—Implications for Air Pollution Research. *Remote Sens.* **2018**, *10*, 978. [[CrossRef](#)]
38. Carslaw, D.C. *The Open Air Manual—Open-Source Tools for Analysing Air Pollution Data*; Manual for Version 2.6-6; University of York: York, UK, 2019.
39. Zeng, Y.; Hopke, P. A study of the sources of acid precipitation in Ontario, Canada. *Atmos. Environ.* **1989**, *23*, 1499–1509. [[CrossRef](#)]
40. Hsu, Y.; Holsen, T.M.; Hopke, P.K. Comparison of hybrid receptor models to locate PCB sources in Chicago. *Atmos. Environ.* **2003**, *37*, 545–562. [[CrossRef](#)]
41. Reddington, C.; Morgan, W.; Darbyshire, E.F.; de Brito, J.; Coe, H.; Artaxo, P.; Marsham, J.; Spracklen, D. Biomass burning aerosol over the Amazon: Analysis of aircraft, surface and satellite observations using a global aerosol model. *Atmos. Chem. Phys. Discuss.* **2018**, *19*, 9125–9152. [[CrossRef](#)]
42. Artaxo, P.; Rizzo, L.V.; Brito, J.F.; Barbosa, H.M.J.; Arana, A.; Sena, E.T. Atmospheric aerosols in Amazonia and land use change: From natural biogenic to biomass burning conditions. *Faraday Discuss.* **2022**, *165*, 203–235. [[CrossRef](#)] [[PubMed](#)]
43. Fernandes, K.; Santos, E.; Godoi, R.; Yamamoto, C.; Barbosa, C.; Souza, R.; Machado, C. Characterization, Source Apportionment and Health Risk Assessment of PM_{2.5} for a Rural Classroom in the Amazon: A Case Study. *J. Braz. Chem. Soc.* **2020**, *32*, 363–375. [[CrossRef](#)]
44. Li, Y.; Tong, D.; Ma, S.; Freitas, S.R.; Ahmadov, R.; Sofiev, M.; Zhang, X.; Kondragunta, S.; Kahn, R.; Tang, Y.; et al. Impacts of estimated plume rise on PM_{2.5} exceedance prediction during extreme wildfire events: A comparison of three schemes (Briggs, Freitas, and Sofiev). *Atmos. Chem. Phys.* **2023**, *23*, 3083–3101. [[CrossRef](#)]
45. Ahangar, F.; Pakbin, P.; Hasheminassab, S.; Epstein, S.; Li, X.; Polidori, A.; Low, J. Long-Term Trends of PM_{2.5} and its Carbon Content in the South Coast Air Basin: A Focus on the Impact of Wildfires. *Atmos. Environ.* **2021**, *255*, 118431. [[CrossRef](#)]
46. Kim, Y.P.; Lee, G. Trend of Air Quality in Seoul: Policy and Science. *Aerosol Air Qual. Res.* **2018**, *18*, 2141–2156. [[CrossRef](#)]
47. Gonzalez-Alonso, L.; Martin, M.V.; Kahn, R. Biomass-burning smoke heights over the Amazon observed from space. *Atmos. Chem. Phys.* **2019**, *19*, 1685–1702. [[CrossRef](#)]
48. Schneider, S.R.; Lee, K.; Santos, G.; Abbott, J.P.D. Air Quality Data Approach for Defining Wildfire Influence: Impacts on PM_{2.5}, NO₂, CO, and O₃ in Western Canadian Cities. *Environ. Sci. Technol.* **2021**, *55*, 13709–13717. [[CrossRef](#)]
49. Global Forest Watch. Available online: <https://www.globalforestwatch.org/dashboards/country/BRA/> (accessed on 7 August 2023).
50. Beuchle, R.; Achard, F.; Bourgoïn, C.; Vancutsem, C. Deforestation and Forest Degradation in the Amazon. Available online: https://publications.jrc.ec.europa.eu/repository/bitstream/JRC130081/JRC130081_01.pdf (accessed on 15 August 2023).
51. Dos Reis, M.; Graça, P.M.L.A.; Yanai, A.M.; Ramos, C.J.P.; Fearnside, P.M. Forest fires and deforestation in the central Amazon: Effects of landscape and climate on spatial and temporal dynamics. *J. Environ. Manag.* **2021**, *288*, 112310. [[CrossRef](#)]
52. Cano-Crespo, A.; Traxl, D.; Thonicke, K. Spatio-temporal patterns of extreme fires in Amazonian forests. *Eur. Phys. J. Spec. Top.* **2021**, *203*, 3033–3044. [[CrossRef](#)]
53. Melecio-Vázquez, D.; Lautenberger, C.; Hsieh, H.; Amodeo, M.; Porter, J.R.; Wilson, B.; Pope, M.; Shu, E.; Waeselynck, V.; Kearns, E.J. A Coupled Wildfire-Emission and Dispersion Framework for Probabilistic PM_{2.5} Estimation. *Fire* **2023**, *6*, 220. [[CrossRef](#)]
54. Rogers, H.M.; Ditto, J.C.; Gentner, D.R. Evidence for impacts on surface-level air quality in the northeastern US from long-distance transport of smoke from North American fires during the Long Island Sound Tropospheric Ozone Study (LISTOS) 2018. *Atmos. Chem. Phys.* **2020**, *20*, 671–682. [[CrossRef](#)]
55. Freeborn, P.H.; Jolly, W.M.; Cochrane, M.A.; Roberts, G. Large wildfire driven increases in nighttime fire activity observed across CONUS from 2003–2020. *Remote Sens. Environ.* **2022**, *268*, 112777. [[CrossRef](#)]
56. Liang, Y.; Jen, C.N.; Weber, R.J.; Misztal, P.K.; Goldstein, A.H. Chemical composition of PM_{2.5} in October 2017 Northern California wildfire plumes. *Atmos. Chem. Phys.* **2021**, *21*, 5719–5737. [[CrossRef](#)]
57. Jaffe, D.A.; O’Neill, S.M.; Larkin, N.K.; Holder, A.L.; Peterson, D.L.; Halofsky, J.E.; Rappold, A.G. Wildfire and prescribed burning impacts on air quality in the United States. *J. Air Waste Manag. Assoc.* **2020**, *70*, 583–615. [[CrossRef](#)] [[PubMed](#)]

58. Liu, Z.; Shen, L.; Yan, C.; Du, J.; Li, Y.; Zhao, H. Analysis of the Influence of Precipitation and Wind on PM_{2.5} and PM₁₀ in the Atmosphere. *Adv. Meteorol.* **2020**, *13*, 5039613. [[CrossRef](#)]
59. Sarangi, C.; Qian, Y.; Leung, L.R.; Zhang, Y.; Zou, Y.; Wang, Y. Projected increases in wildfires may challenge regulatory curtailment of PM_{2.5} over the eastern US by 2050. *Atmos. Chem. Phys.* **2023**, *23*, 1769–1783. [[CrossRef](#)]

Disclaimer/Publisher’s Note: The statements, opinions and data contained in all publications are solely those of the individual author(s) and contributor(s) and not of MDPI and/or the editor(s). MDPI and/or the editor(s) disclaim responsibility for any injury to people or property resulting from any ideas, methods, instructions or products referred to in the content.